Seismic and radar tomography of a Maya pyramid ruin

Matthew D. Allen and Robert R. Stewart

ABSTRACT

A number of seismic surveys, in addition to a ground penetrating radar (GPR) test, have been conducted on a Maya pyramid ruin at the Maax Na archaeological site in Belize, Central America. The pyramid stands some 15 m high with an approximate 28 m by 28 m base. The purpose of these surveys was to determine whether seismic and GPR tomography techniques could be used to create images of the pyramid's carbonate rubble interior. We find that hammer seismic and GPR waves can be transmitted through the pyramid. Transmitted wave traveltimes were picked for all the surveys and used in a traveltime inversion to create velocity maps of the interior.

Two different approaches were used to find the velocity structure. A straight ray approach successfully solved for velocity models with average traveltime residuals (measured minus calculated) measuring approximately 1.6 ms for the seismic surveys and 2.9 ns for the GPR surveys. The curved ray technique solved for a velocity model with improved average residuals for the lower seismic survey of approximately 1.5 ms. However, the average residuals increased for both the upper seismic and GPR survey to values of approximately 3.9 and 4.3 respectively. This method produced no unphysical values but tight velocity constraints had to be implemented.

INTRODUCTION

Tomography is beginning to be used to assist archaeologists in mapping ancient structures and their foundations (Merlanti and Musante, 1994; Polymenakos and Papamarinopoulus, 2005; ibid, 2007; Schicht et al., 2007). Archaeologists often concentrate on detailed excavations on the order of a few meters at a time. These excavations are both costly and time consuming as well as invasive. To better manage some of this effort, tomographic techniques can be used as a relatively fast and inexpensive way of determining interior or subsurface properties. This might allow archaeologists to better direct their excavation to more promising areas and potentially avoid regions of less significance.

In 2002, two hammer seismic surveys were acquired around a Maya pyramid in Belize at the Maax Na archaeological site. The goal of these tests was to determine whether seismic energy would transmit through the structure (thereby allowing an internal image to be reconstructed). The pyramid consists of carbonate runnel and mortar covered with a loose layer of jungle detritus and is approximately 28 m by 28 m at the base with a height of 15 m (Figure 1). In the first survey, sixty vertical geophones were planted around the lower circumference of the pyramid with a 2 m geophone spacing. Sixty-one sledgehammer source points were placed between the geophones. The second survey was placed around a circumference further up the pyramid. A geophone spacing of 1m with source points spaced between was used.

In 2008, we returned to the site of Maax Na and acquired a GPR survey around a portion of the pyramid's circumference. The GPR survey was acquired using Sensors and

Software's pulse EKKO Pro using 100MHz antennas. A total of eight different transmitter locations were used along a 30 meter line with 151 different receiver locations spaced every 0.2 meters.

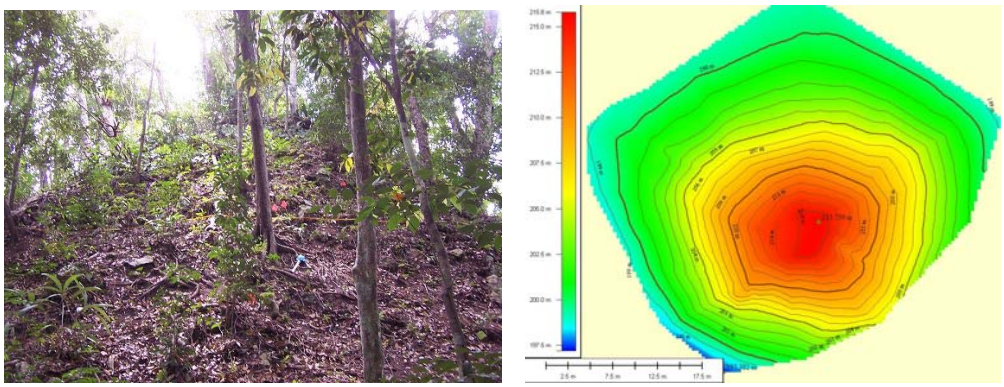

FIG. 1. View (left) and contour map (right) of the Maya pyramid at the Maax Na archaeological site, Belize (contour map courtesy of Henry Bland).

INVERSION METHODS

Both straight and curved ray tomography techniques were used to solve for the velocity structures of both the seismic and GPR surveys. When solving the straight ray inversions the conjugate gradient method (see Yilmaz, 2001) was used with a total of 30 iterations. The curved ray inversion solved for the velocity structure using the 2Dray_tomo program created by Zhou et al. (1992a). This program uses the minimum traveltime method of Moser, (1991) and Zhou et al., (1992a). This method uses a number of nodes on the grids that are connected to create the shortest path between source and receiver as well as a fast and efficient damping L2-norm inversion algorithm (Zhou, 1992b). For all the surveys the maximum amount of 25 nodes per grid were used along with a damping factor of $1x10^{-6}$.

SEISMIC TOMOGRAPHY

Lower Survey

The sledgehammer source was struck once per shot location producing a signal ranges from approximately 5-200 Hz with some shots as high as 300 Hz (Figure 2). The lower survey had 52 sources and 54 receivers usable (Figure 3). Several receivers and sources were ignored due to their position off the vertical contour. Since the survey is solved as a 2D slice all sources must remain in the same plane. Other source and receiver locations were ignored due to unsafe conditions or faulty equipment. This provided for a total of 2808 rays to be used in the inversion. The first break traveltimes were picked to be used in the traveltime inversion.

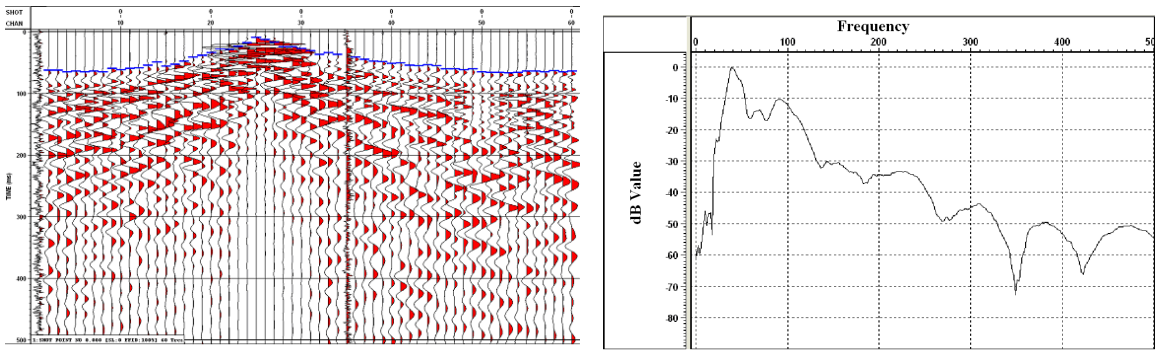

FIG. 2. A sample shot with a 500ms AGC with first breaks show in blue (left) and the amplitude spectrum of the average data trace for the shot (right).

When solving for the velocity structure for the seismic surveys, a grid size of 1m by 1m was used for both the straight and curved ray techniques. This size provided for a large fold (rays crossing per pixel) while still remaining small enough to provide interesting detail.

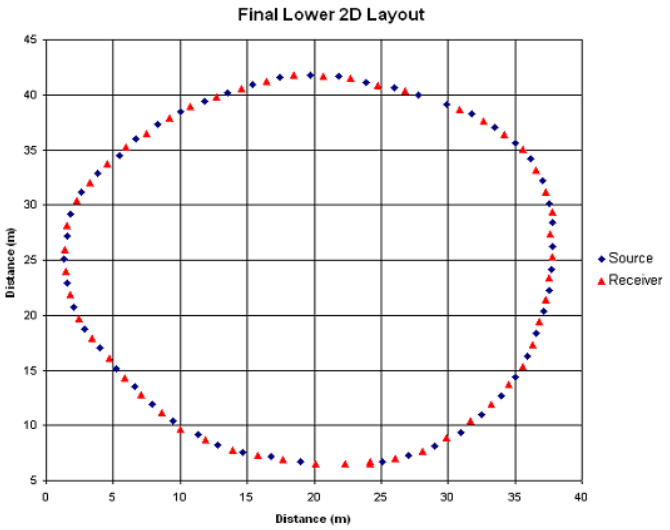

FIG. 3. The source and receiver layout for the lower seismic survey. Sources are displayed in blue and receivers in red.

The derived velocity structure found using straight ray inversion resulted in several negative values. Since these negative values are not physical they were set equal to zero. Along with the negative values there were a few velocity values that appeared to be too high to be physical. These velocities were set equal to 3000 m/s. The final velocity structure can be seen in Figure 4.

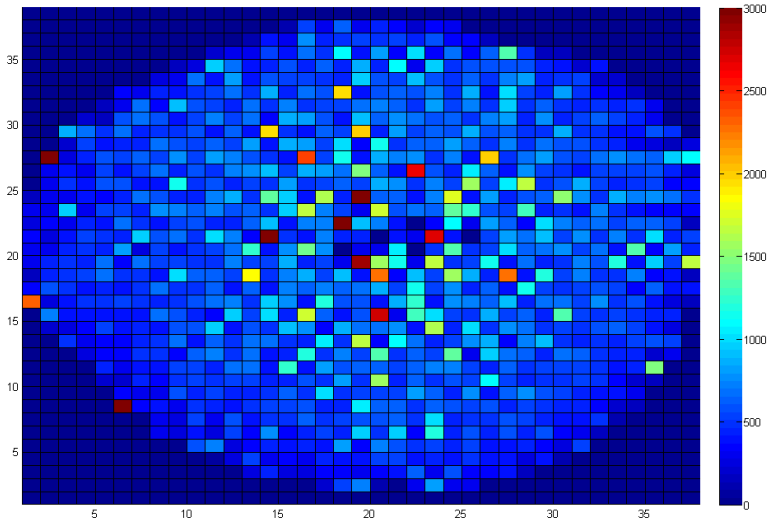

FIG. 4. The final velocity (m/s) map of the Maax Na pyramid found using straight ray tomography. All negatives values have been set equal to zero all velocities greater than 3 km/s set to 3 km/s.

To find the most accurate velocity model possible with the curved ray tracer multiple velocity constraints were tried before selecting a constant velocity model of 500 m/s with velocity constraints of 1 m/s to 2000 m/s. This velocity resulted in the lowest average differences in traveltimes as well as the lowest standard deviations. A total of 150 iterations were undertaken to find the minimum average differences. Upon comparison iteration 90 proved to give the best velocity model as shown in Figure 5.

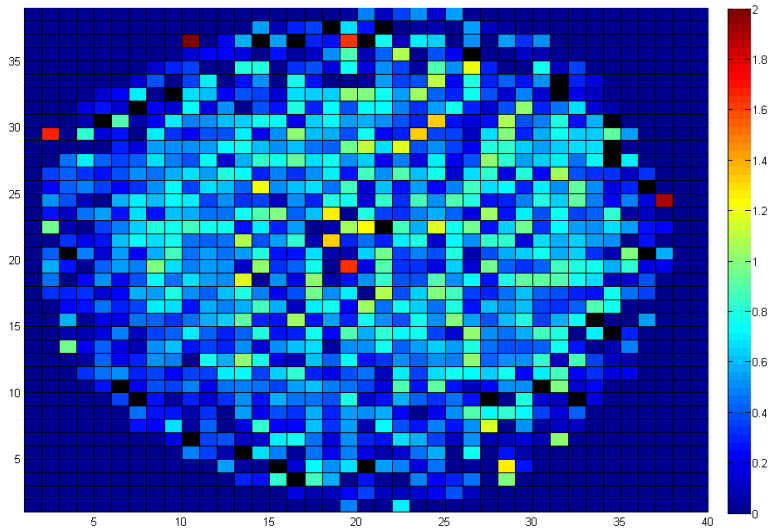

FIG. 5. The derived curved ray velocity model (km/s) of the lower survey found using a curved rays and a velocity range of 0.001 to 2.0 km/s. Skipped pixels are designated in black.

A new set of traveltimes was derived based on the modeled velocity structures found by the straight and curved ray tracing. The negative and high velocity values were included in straight ray model. The derived traveltimes were then compared to the original first break traveltime picks. The results can be seen in Figure 6. The differences

graph shows that the curved ray differences are more closely bunch around zero then those of the straight ray differences.

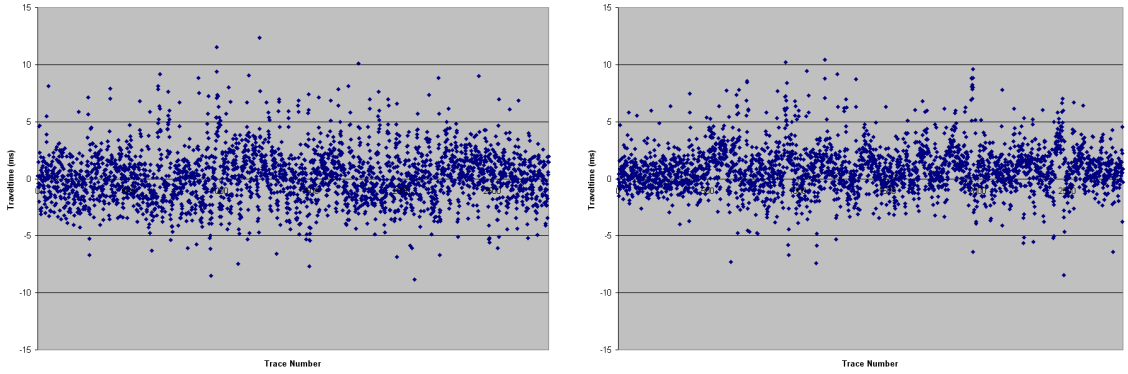

FIG. 6. Differences between measured and calculated traveltimes found for the lower survey using straight (left) and curved (right) ray tracing.

The standard deviation and the average of the absolute values of the traveltime differences were derived to help determine the accuracy of the velocity model. The average and standard deviation values are 1.63 ms and 2.34 ms respectively for the straight ray model and 1.56 ms and 1.97 ms for the curved ray model. The curved ray model appears to give the better results as was expected since the rays are allowed to bend making them more realistic. The straight ray model does have similar average and standard deviation values and displays a similar velocity model. Both models displayed a slowly increasing velocity model from the exterior to the interior with a small unstable velocity region in the center. The unstable velocity region could be the result of a small cavity in the interior or the remains of a previous structure on which the pyramid was built.

Upper Survey

Due to the spacing size there were not enough geophones to cover the full circumference, therefore one side is left open (Figure 7). Inside this open side is an empty looters' trench. Since the rays will be affected by this empty space all rays passing through this trench were ignored in the straight ray inversion. Therefore instead of the initial 3660 rays only 3054 rays were used. In addition to removing the rays an initial velocity model with the trench area removed was used in the curved ray. This insures that the remaining rays do not pass through the location of the trench.

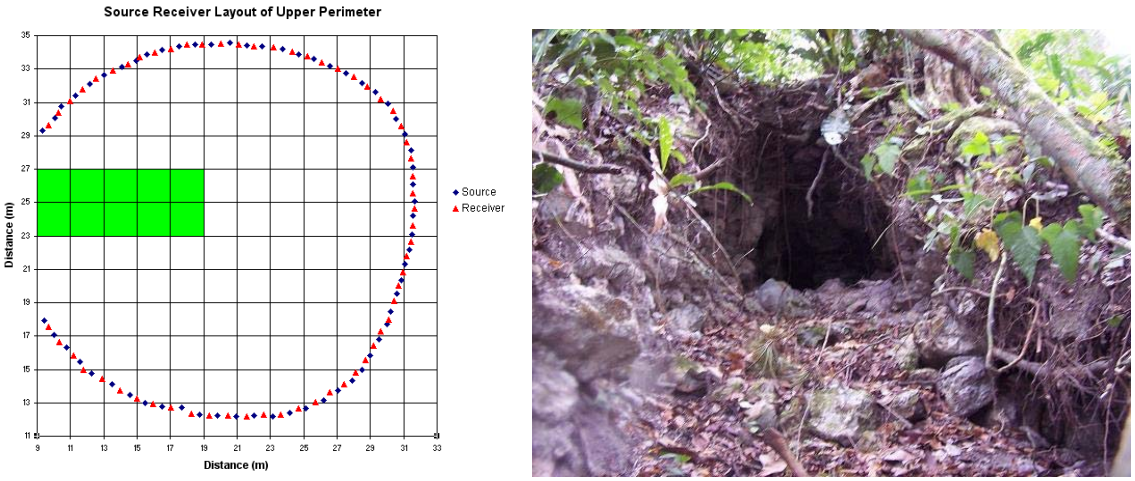

FIG. 7. The source and receiver layout for the upper perimeter of the Maax Na pyramid (left) with the looters trench (right) displayed in green.

As before, the sledgehammer was swung once per shot point and a grid size of 1m by 1m was used. Again, the first break traveltimes were used to create the velocity profiles. A number of unphysical values were derived in the straight ray inversion. The negative velocities were set equal to 0 m/s and the high velocities were set equal to 3000 m/s. The straight ray inversion results can be seen in Figure 8.

As with the lower seismic survey many different velocity constraints were attempted in order to derive the most accurate velocity model. Based on the standard deviations and averages of the differences between the measured and calculated traveltimes the 0.15 to 0.5 km/s velocity range proved to provide the most accurate model. Solving for a total of 150 iterations, the 3rd iteration had the smallest average difference and was chosen as the most accurate model. The final velocity model found through curved ray inversion is shown in Figure 9.

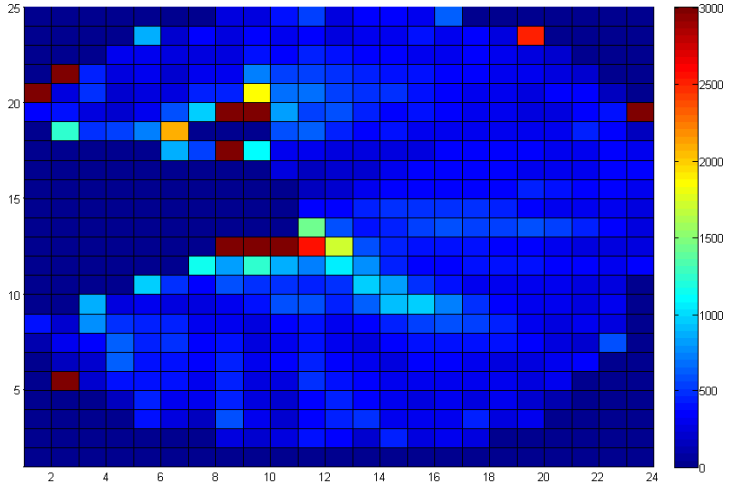

FIG. 8. The straight ray velocity (m/s) model of the upper survey found when all rays passing through the trench had been removed. All velocity values >3000m/s have been set =3000m/s. All negative values are set =0.

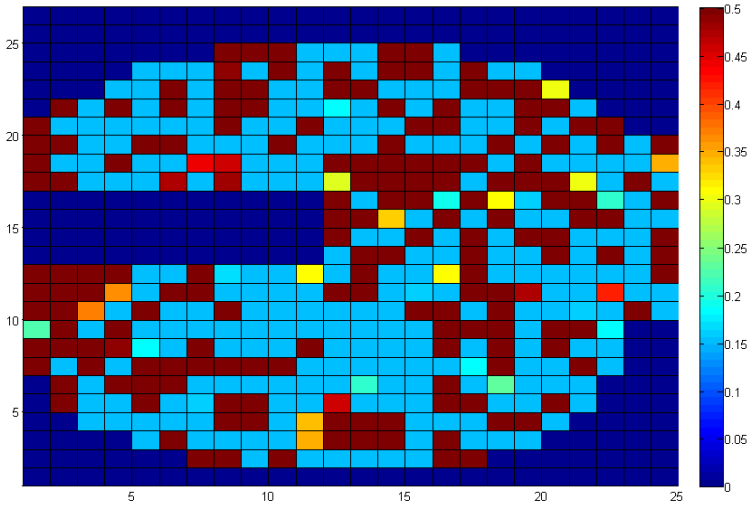

FIG. 9. The curved ray velocity model (km/s) of the upper survey found using velocity constraints of 0.15 to 0.5 km/s and an initial velocity model of 0.5 km/s with the trench region removed.

The differences between the observed and calculated traveltimes were again derived for both the straight and curved ray model and are displayed in Figure 10. The differences appear to be much better for the straight ray model then the curved ray model. The average and standard deviations of the differences also appear to be displaying an advantage for the straight ray model. The averages and standard deviations were found to be 1.603 ms and 2.114 ms for the straight ray model and 3.897 ms and 4.718 ms for the curved ray model. While the differences are significant the curved ray model does not have any unphysical values whereas the straight ray model does. Both models do show similarities with a fairly homogenous low velocity interior. As the interior appears to be homogenous there does not appear to be any objects of archaeological significance inside the upper survey.

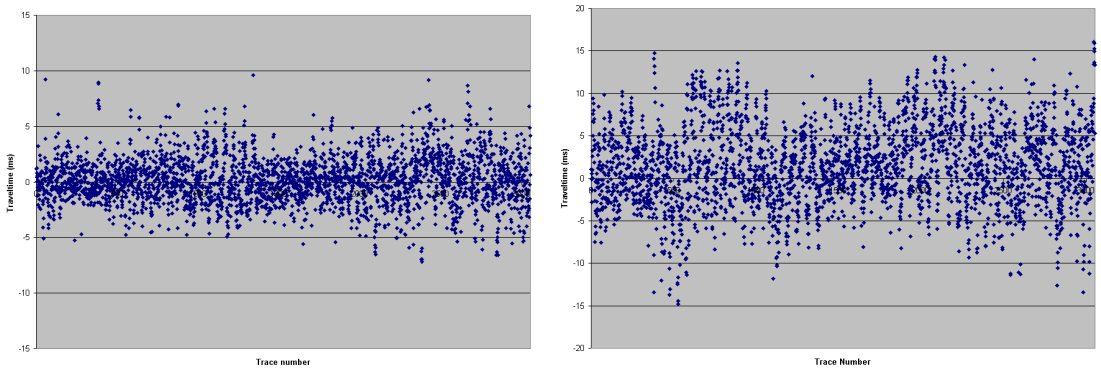

FIG. 10. Differences between measured and calculated traveltimes found for the upper survey using straight (left) and curved (right) ray tracing.

GPR TOMOGRAPHY

Unlike the seismic surveys, the direct transmission in a ground-penetrating radar measurement is not the first arrival measurement observed on the shot gather. Instead an airwave will typically arrive first. This airwave must be ignored and the transmitted wave

found. A raw shot gather from this survey can be seen in Figure 11 with both the air and direct wave indicated. Another problem with the GPR survey at 100 MHz is that the signal may not transmit through the entire pyramid. GPR has a much more limited range than that of seismic therefore some initial processing should be completed in order to see as much of the direct wave as possible. Due to the lack of signal many of the receiver points must be ignored since no traveltime can be found.

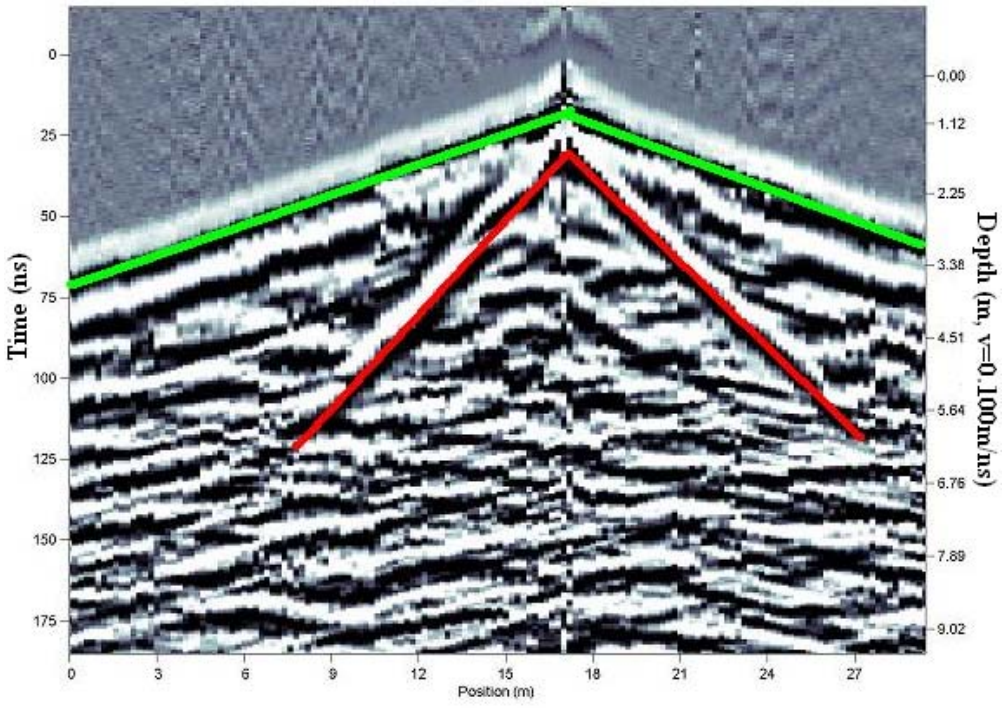

FIG. 12. A raw shot gather from the GPR survey with the airwave marked in green and the transmitted wave marked in red.

The 100 MHz antennae on the pulse EKKO pro system produced on average a relatively broadband signal up to 140 MHz. The peak frequency appears to be approximately 50 MHz for all the shots. An example shot frequency graph can be seen in Figure 11.

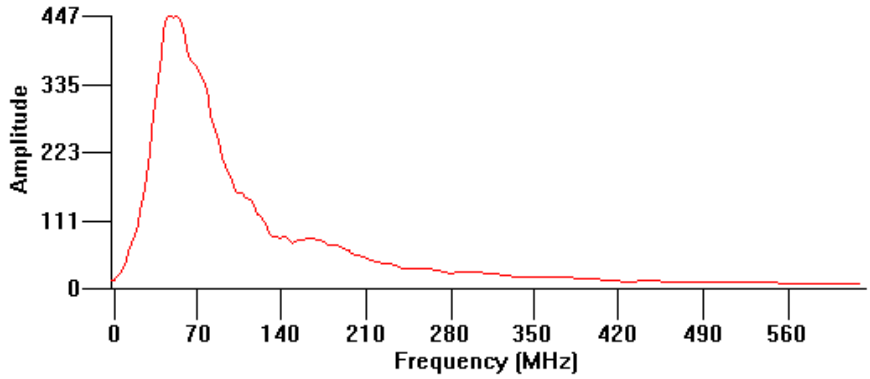

FIG. 11. The amplitude frequency graph for shot 2.

To enhance the transmitted wave an FK filter was used on the shots (Figure 13). By applying the FK filter, a clear view of the transmission wave without the air wave and much of the noise is displayed (Figure 14). This allows for the traveltimes of the transmitted wave to be picked more easily. We see that despite concerns about the depth of penetration the transmitted wave penetrates about ten meters on either side of the shot. When picking the traveltimes multiple receivers were ignored near the shot location due to interference of the airwave and the transmitted wave. Once all reliable picks had been made a total of 735 traveltimes remained.

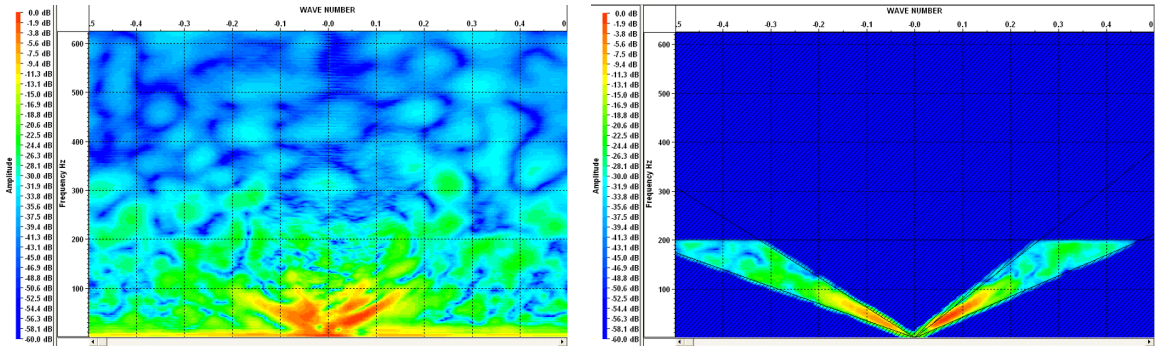

FIG. 13. The initial FK spectrum (left) and final FK spectrum (right) after applying the FK filter.

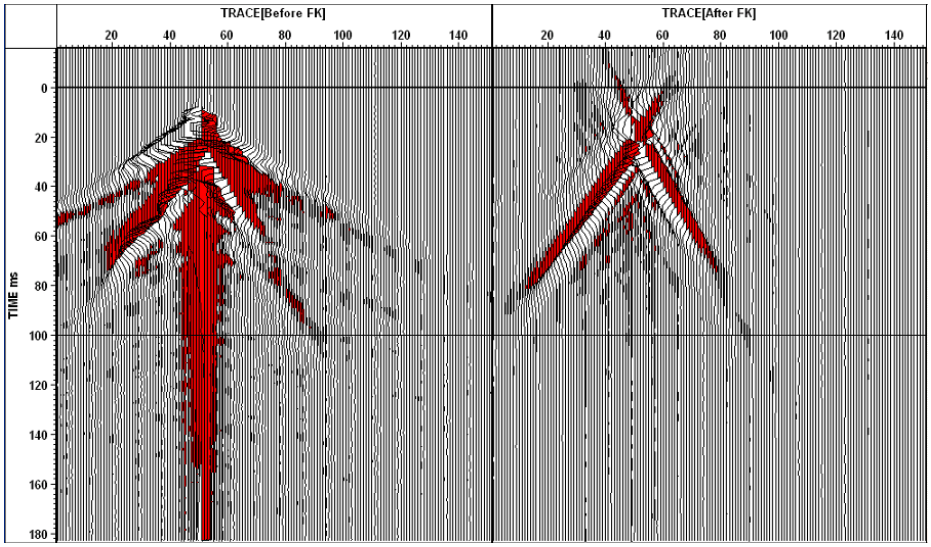

FIG. 14. The raw shot gather (left) and the shot gather after applying the FK filter.

Since the receiver spacing was much smaller then the seismic surveys a smaller grid size of 0.5 m by 0.5 m was used for both the straight and curved ray techniques. Since a large percentage of this GPR survey is covering the loose soil layer, with variable velocities, the smaller grid size will better image this. The smaller grid size does result in a lower fold however; in general this value remains in acceptable levels.

Similar to the seismic surveys, the GPR straight ray velocity model contained multiple unphysical values. Once again all negative velocities were set equal to 0 m/ns. Along with the negative values, multiple unphysical high velocities were also derived and were

set equal to 0.2 m/ns. This value was chosen as a maximum based on GPR surveys previously performed on the plaza area of Maax Na by Aitken and Stewart (2004). In these surveys, velocities were found to range from 0.072 to 0.106 m/ns in wet conditions and 0.122 to 0.140 m/ns in dry conditions. Since the plaza is made of similar carbonate as the pyramid these velocities can provide some guidance for the range of expected values. A maximum velocity of 0.2 m/ns was set as the fill in the pyramid may be less dense then that in the plaza and may result in faster velocities. The final straight ray velocity structure can be seen in Figure 15.

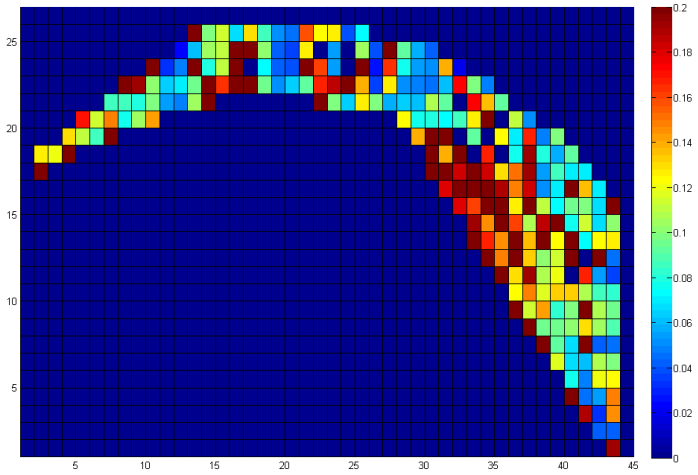

FIG. 15. The final velocity (m/ns) structure derived from straight ray traveltime inversion. All negative values set to 0m/ns. All velocities greater than 0.2 m/ns are set equal to 0.2 m/ns.

After solving for the velocity model using many different velocity constraints the most accurate model was found using the velocity range of 0.07 m/ns to 0.11 m/ns and a 0.1 m/ns constant velocity starting model. Solving 150 iterations using this range the 137th iteration proved to provide the most accurate result. The final curved ray velocity model is displayed in Figure 16.

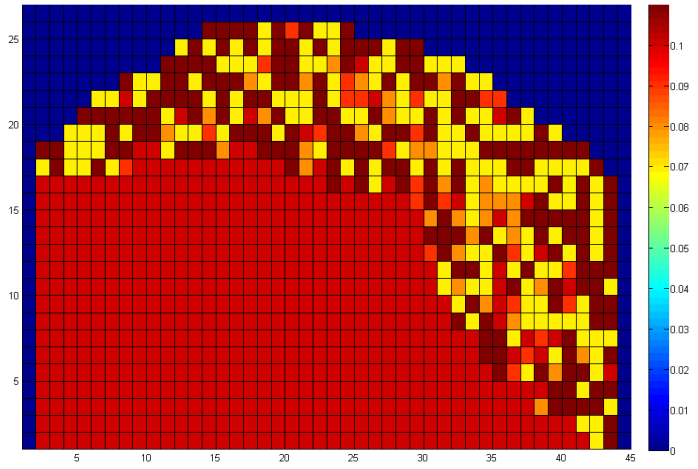

FIG. 16. The final velocity model (m/ns) derived from the curved ray traveltime inversion. Parts of the initial model of 0.1 m/ns remain in areas of no ray coverage.

The differences between the measured and calculated traveltimes (Figure 17) shows similar results with the straight ray model producing slightly lower differences. The averages and standard deviations of 2.942 ns and 3.242 ns for the straight ray model and 4.324 ns and 5.695 ns for curved ray model show the same results with the straight ray model producing lower values. While the straight ray model would appear to be more accurate the curved ray model allows no unphysical values which may result in the curved ray model being more reliable.

Both these difference graphs display regions of large differences. The largest differences in general appear in the rays that have the shortest distance to travel. These are the rays that area expected to have the largest difference as they pass through a limited number of pixels resulting in the rays having limited effect on the total velocity model. Since these rays have such a small distance to travel even a small velocity error can produce a large error in traveltimes.

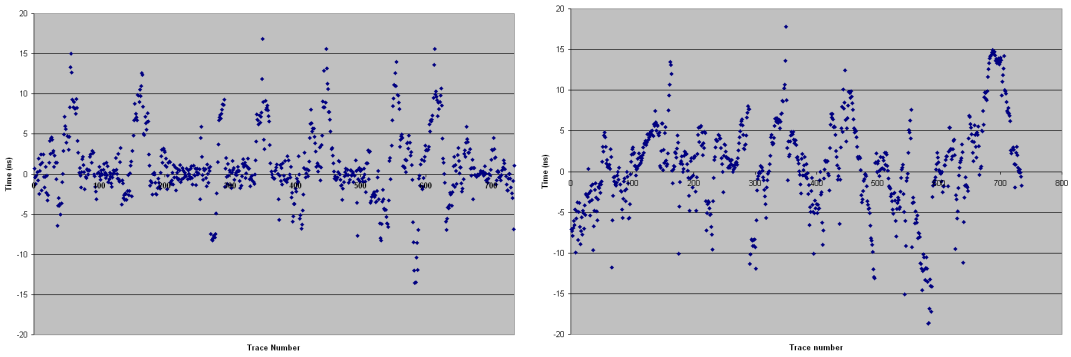

FIG. 17. The difference between the measured and calculated traveltimes of the straight (left) and curved (right) ray GPR survey.

CONCLUSIONS

Seismic tomographic techniques using a hammer source and seismic receivers produced clear shot gathers with easily distinguished first break times. GPR was also capable of penetrating adequate depths. In this survey, a 100 MHz GPR antenna was used and the wave penetrated an approximate distance of 10m on either side of the source point. If a lower frequency antenna was used the penetration distance should increase.

The straight ray traveltime inversions produced velocity models with the majority of velocities in an acceptable range. In both seismic and GPR surveys, straight ray inversion produced several negative as well as excessively high velocities. These negative values tended to be located in areas of low fold. An increase in either source or receiver points should increase the coverage and therefore allow the velocities to further converge.

The curved ray traveltime inversion displayed similar velocity maps as the straight ray inversions for the seismic surveys. When comparing the differences between the measured first break traveltimes and those calculated using the derived model the curved ray model showed an improvement over the straight ray. This was not the case in the upper seismic survey. The average and standard deviation of the traveltime differences dramatically increased from straight ray to curved ray. This would suggest an advantage

with the straight ray method however, when deriving the straight ray model multiple unphysical values were produced. The curved ray allowed a starting velocity model with the location of the trench removed and no unphysical values were derived.

The GPR survey showed a slight advantage in the straight ray model when considering the differences in traveltimes. Once again the curved ray inversion produced no unphysical values and allowed for more realistic ray paths. This may give the advantage to the curved ray technique. The curved ray inversion used tight velocity constraints on both the GPR and upper seismic survey in order to produce an accurate model. In order to increase the accuracy a greater number of source and receiver points must be included, which should allow a widening of the velocity constraints.

Both GPR and seismic proved to be effective methods for performing tomography on large structures. Both straight and curved ray techniques also proved effective for both GPR and seismic by producing similar models.

REFERENCES

Merlanti, F., and Musante, B., 1994, Seismic tomography: application for archaeological purposes: Geoarchaeology, **9**, 317-329.

Moser, T.J., 1991, Shortest path calculation of seismic rays, Geophysics, **56**, 59-67.

Polymenakos, L., and Papamarinopoulus, S. P., 2005, Exploring a prehistoric site for remains of human structures by three-dimensional seismic tomography: Archaeological Prospection, **12**, 221-233.

Polymenakos, L., and Papamarinopoulus, S. P., 2007, Using seismic traveltime tomography in geoarchaeological exploration: an application at the site of Chatby cemeteries in Alexandria, Egypt: Near Surface Geophysics, **5**, 209-219.

Schicht, T., Lindner, U., Heckner, J., Strobel, G., and Rappsilber, I., 2007, Seismic tomography on the castle hill in Quedlinburg: Near Surface Geophysics, **5**, 339-343.

Yilmaz, O., 2001, Seismic data analysis: processing, inversion and interpretation of seismic data. Vol. 2. Society of Exploration Geophysicists.

Zhou, B., Sinadinovski, C. and Greenhalgh, S.A., 1992, Non-linear inversion travel-time tomography: imaging high-contrast inhomogeneities, Exploration Geophysics, **23**, 459-464.

Zhou, B., Greenhalgh, S.A., and Sinidinovski, C., 1991, Iterative algorithm for the damping minimum norm, least squares and constrained problem in seismic tomography, Exploration Geophysics, **23**, 497-505.